

## Searching for high-spin toroidal isomers in collisions induced by $\alpha$ -conjugate nuclei

X.G. Cao, K. Schmidt, E.-J. Kim, K. Hagel, M. Barbui, J. Gauthier, M. Huang, J.B. Natowitz,  
R. Wada, S. Wuenschel, G.Q. Zhang, H. Zheng, N. Blando, A. Bonasera,  
G. Giuliani, M. Rodrigues, C. Botosso, and G. Liu

Nuclei in the valley of stability are usually treated as a fluid made of nucleons with sphere-like geometry in their ground states. However, correlations between nucleons and cluster formation play more important roles in excited nuclei. For light excited  $\alpha$ -conjugate (even-even  $N=Z$ ) nuclei, the importance of  $\alpha$  clusters is apparent in both theoretical calculations and experimental observables.

Wheeler suggested that nuclear liquid can assume toroidal shapes under certain conditions [1]. Wong et al. quantitatively discussed where the existence of a toroidal nucleus and its stability against sausage deformation [2, 3]. In light  $\alpha$ -conjugate nuclei the  $\alpha$  particle can be expected to be important in the toroidal configuration which leads to a reduced nuclear density. Heavy ion collisions induced by light  $\alpha$ -conjugate nuclei may provide the appropriate conditions to access toroidal isomers with high angular momentum and excitation energy. The toroidal isomer may manifest itself by decaying into  $\alpha$  particles or  $\alpha$ -like fragments (where the  $\alpha$ -like fragments refer to  $\alpha$ ,  $^{12}\text{C}$ ,  $^{16}\text{O}$ , and  $^{20}\text{Ne}$  etc.). Therefore, an experimental exploration with special attention and methodology into observing  $\alpha$ -like decays is indicated and very intriguing.

A series of experiments were carried out at Texas A&M University Cyclotron Institute with  $^{40}\text{Ca}$  and  $^{28}\text{Si}$  beams at 10, 25, 35 MeV/u provided by the K500 superconducting cyclotron incident on  $^{28}\text{Si}$ ,  $^{12}\text{C}$ ,  $^{40}\text{Ca}$ , and  $^{181}\text{Ta}$  targets [4], respectively. The combinations with different  $\alpha$ -conjugate projectiles ( $^{28}\text{Si}$  and  $^{40}\text{Ca}$ ) and targets ( $^{12}\text{C}$ ,  $^{28}\text{Si}$ , and  $^{40}\text{Ca}$ ) may favor population of different  $\alpha$  cluster states. The reaction products were detected using a  $4\pi$  array, NIMROD-ISiS (Neutron Ion Multidetector for Reaction Oriented Dynamics with the Indiana Silicon Sphere), which consisted of 14 concentric rings covering from  $3.6^\circ$  to  $167^\circ$  in the laboratory frame. In addition, the neutron ball surrounding the NIMROD-ISiS charged particle array provided information on average neutron multiplicities for different selected event groups. The preliminary analysis of parts of the raw data was accomplished by C. Bottosso, E-J Kim, and K. Schmidt *et al.* [4] and some interesting preliminary results about the  $\alpha$ -like mass (Almass) emission have been obtained for  $^{40}\text{Ca}+^{40}\text{Ca}$  [5]. Here we focus on cluster decay from  $^{28}\text{Si}$  and check its dependence on  $^{12}\text{C}$ ,  $^{28}\text{Si}$  and  $^{181}\text{Ta}$  targets [6].

For the  $^{28}\text{Si}+^{12}\text{C}$  reaction, a total of 17 million events were recorded and a significant proportion of events have significant alpha-like mass emission. Half a million events have Almass=28. There are 7 alpha-like decay channels with Almass=28 as shown in Fig. 1. For the most interesting event group: 7  $\alpha$  decay channels, more than 10 thousand events are obtained.

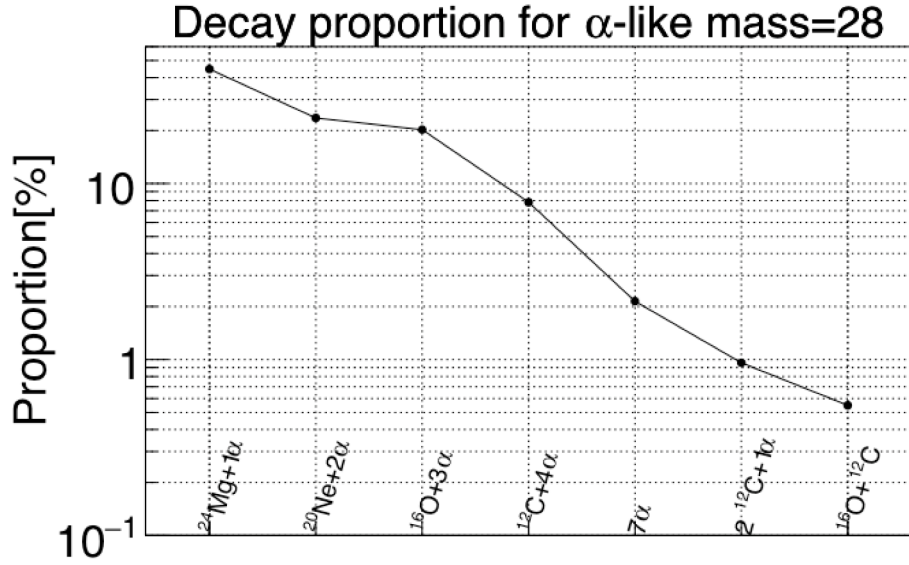


FIG. 1. The proportion of decay channels for  $A_{\text{mass}}=28$  from  $^{28}\text{Si} + ^{12}\text{C}$  @ 35MeV/u.

The hierarchy effect, which refers to a correspondence between fragment mass and parallel velocity, was found for  $\alpha$ -like fragments from  $^{40}\text{Ca}$  decay [5]. For most of the  $^{28}\text{Si}$  channels this hierarchy effect is also observed. The angles between  $\alpha$  and heavier fragments are shown in Fig. 2. The  $\alpha$ s tend to

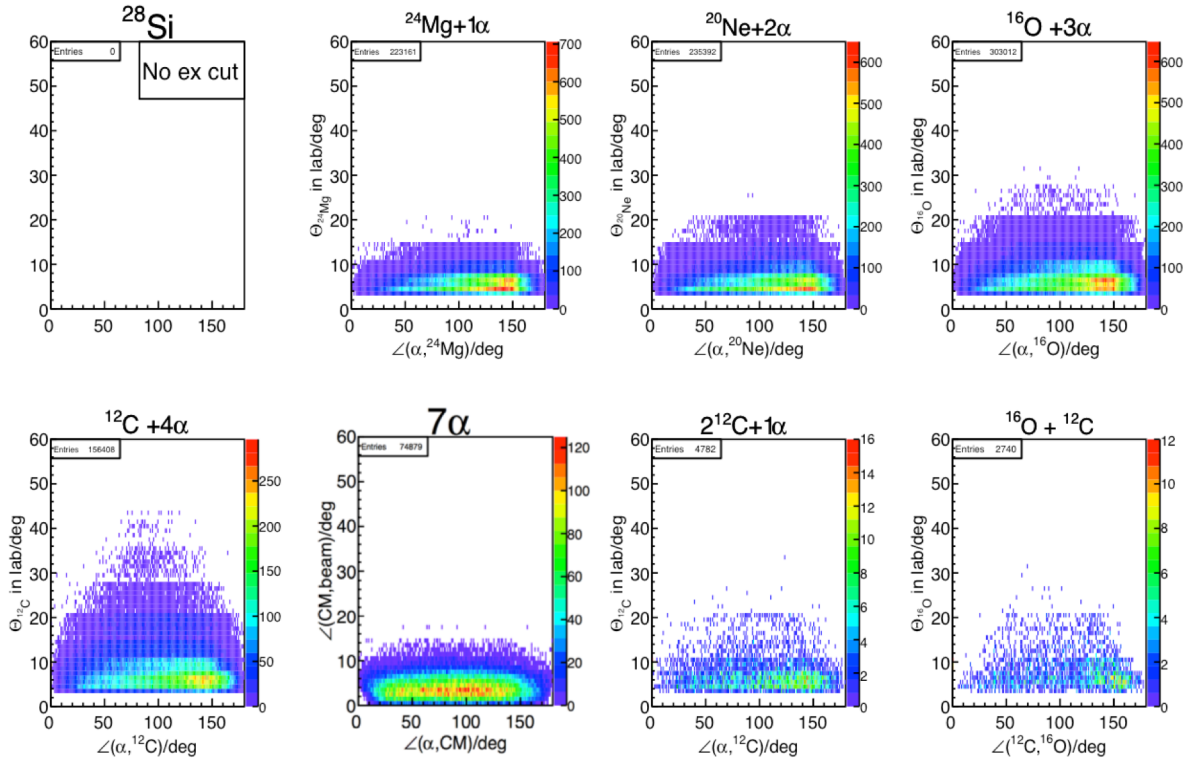
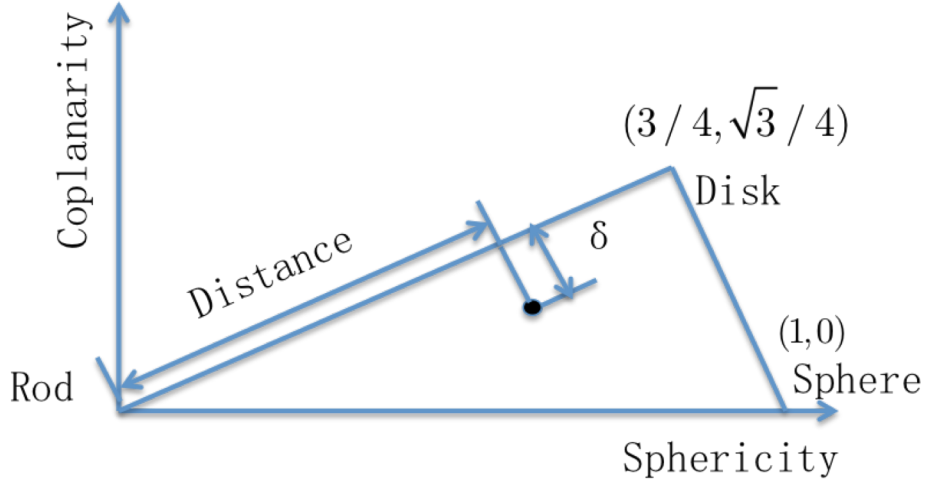


FIG. 2. The emission angle between  $\alpha$  and heavier fragment for the  $\alpha$ -like decay channels. For the  $7\alpha$  channel, the angle is calculated between center-of-mass velocity and the velocity of  $\alpha$  particles.

be emitted backward relative to the large fragment, indicating they mainly come from the neck region. This means absence of complete equilibrium of the  $\alpha$ -like emission source.

In order to explore the configuration of the possible toroid formed in the dynamical stage, we utilize a shape analysis technique to diagnose the source shape in momentum space [7]. Shape analysis is a popular method to study emission patterns of sources, dynamical aspects of multifragmentation and collective flows of particles in relativistic heavy ion collisions. A tensor constructed on the momenta can be written as:  $T_{ij} = \sum_{\nu=1}^N p_i^\nu p_j^\nu$ , where N is the total nucleon number,  $p_i^\nu$  is the momentum component of  $\nu^{\text{th}}$  nucleon in the center-of-mass and i refers to the Cartesian coordinate. The tensor can be diagonalized to reduce the event shape to an ellipsoid. The eigenvalues of the tensor:  $\lambda_1, \lambda_2$ , and  $\lambda_3$ , normalized by:  $\lambda_1 + \lambda_2 + \lambda_3 = 1$  and ordered according to:  $\lambda_1 \leq \lambda_2 \leq \lambda_3$ , can quantitatively give shape information of the events. The sphericity is defined as:  $S = \frac{3}{2} (1 - \lambda_3)$ , and coplanarity is defined as:  $S = \frac{\sqrt{3}}{2} (\lambda_2 - \lambda_1)$ . In the sphericity-coplanarity plane, the ideal rod, disk and sphere events exactly locate at the three vertexes of the triangle: (0,0) (3/4,  $\sqrt{3}/4$ ), and (1,0), respectively. A schematic figure of shape analysis is shown by Fig. 3.



**FIG. 3.** A schematic figure illustrating the shape analysis method, where the  $\delta$  and distance definitions are used in Fig. 5.

The results of the shape analysis are shown in Fig. 4. events. Two fragments will always have a rod shape in momentum space while three fragments can form a plane or rod shape. We can see there are always some events located around the disk point, which may be the toroidal candidates, especially for the 7  $\alpha$  channel.

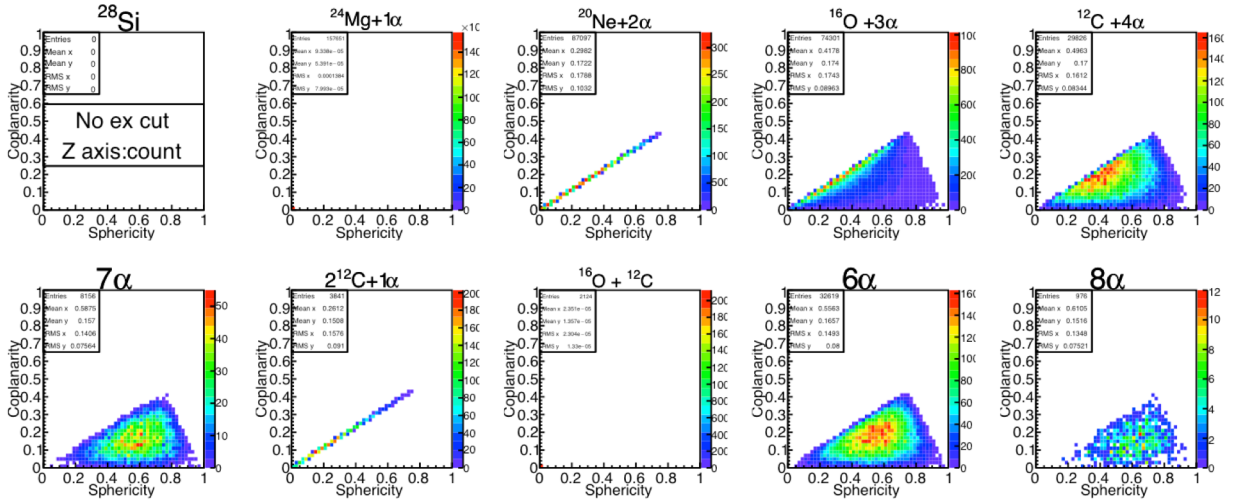


FIG. 4. Shape analysis of sources decaying by Almass.

We extract the excitation energy of source decaying by Almass by scanning around the rod-disk line. The extracted excitation energy is shown in Fig. 5, with cut labeled:  $\delta \in [0,0.05]$  and  $distance \in [0.4,0.6]$ , where the  $\delta$  and distance are defined in Fig. 3. For our most interesting channel:  $7\alpha$ , there are several peaks near the 143.18 MeV energy predicted by Staszczak and Wong's [3]. They predicted this to be a  $44\hbar$   $^{28}\text{Si}$  isomer corresponding to a toroidal configuration. The  $6\alpha$  and  $8\alpha$  channels are included for comparison. For the  $6\alpha$  channel, there are no obvious peaks. For the  $8\alpha$  channel, at least one  $\alpha$  would have to come from the target-like fragment (TLF). The statistics are low and this suggests that the  $7\alpha$  we analyzed may be relatively free of contributions from decay of the target-like fragment (TLF).

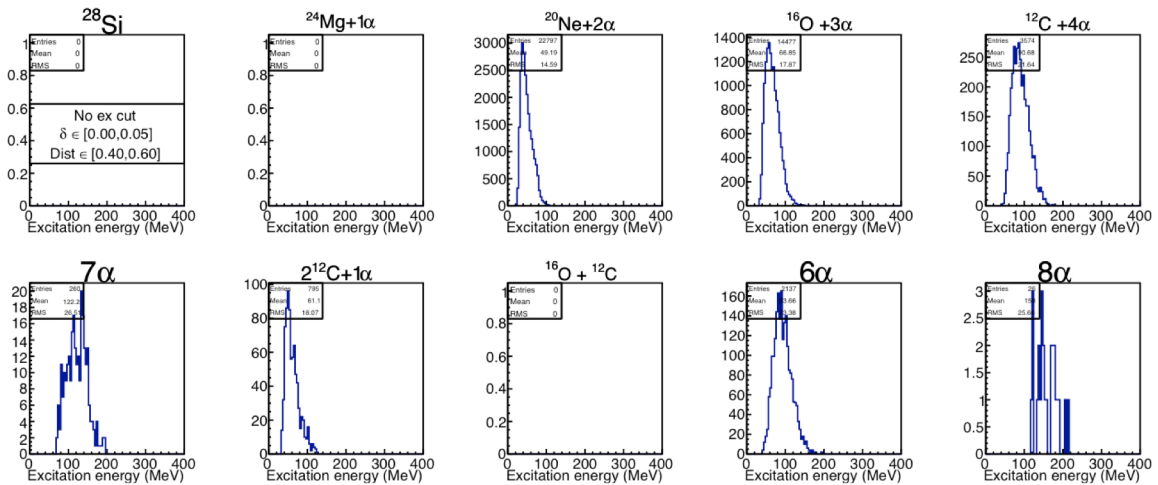


FIG. 5. Excitation energy of Almass source with cut on sphericity-coplanarity plane.

A determination of the angular momentum of Almass source is necessary to pin down the toroidal candidate. Such a determination is difficult. Antisymmetrized molecular dynamics (AMD) simulations are in progress.

Similar results are seen for the  $^{28}\text{S}+^{28}\text{Si}$ , and  $^{28}\text{Si}+^{181}\text{Ta}$  systems at 35MeV/u. However, the statistics for the  $^{28}\text{Si}+^{181}\text{Ta}$  reaction is much lower than for the other two systems.

- [1] G. Gamow, *Biography of Physics*, Harper & Brothers Publishers, New York, 1961, 297 pp.
- [2] C.Y. Wong, *Phys. Lett.* **41B**, 446 (1972); C.Y. Wong, *Phys. Rev. C* **17**, 331 (1978).
- [3] A. Staszczak, C.Y. Wong, *Phys. Lett. B* **738**, 401 (2014).
- [4] K. Schmidt *et al.*, *Progress in Research*, Cyclotron Institute, Texas A&M University (2010-2011), p. II-8; C. Bottosso *et al.*, *Progress in Research*, Cyclotron Institute, Texas A&M University (2008-2009), p.II-7.
- [5] K. Schmidt *et al.*, *Progress in Research*, Cyclotron Institute, Texas A&M University (2011-2012), p. II-7; *Progress in Research*, Cyclotron Institute, Texas A&M University (2012-2013), p. II-17; *Progress in Research*, Cyclotron Institute, Texas A&M University (2013-2014), p. II-18.
- [6] X.G. Cao *et al.*, *Progress in Research*, Cyclotron Institute, Texas A&M University (2014-2015), p. II-16.
- [7] J. P. Bondorf *et al.*, *Phys. Lett. B* **240**, 28 (1990).